Crustal structure beneath Istra peninsula based on receiver function analysis

Jasna Orešković[1], Franjo Šumanovac[1] and Endre Hegedűs[2]

[1]University of Zagreb, Faculty of Mining, Geology and Petroleum Engineering, Zagreb, Croatia

[2]Eötvös Loránd Geophysical Institute of Hungary, Budapest, Hungary

The structure of the Earth's crust has been determined at three temporary seismic stations in Istra (Croatia) installed as a part of the passive seismic experiment ALPASS-DIPS (**A**lpine **L**ithosphere and Upper Mantle **PAS**sive **S**eismic Monitoring – **DI**narides-**P**annonian **S**egment). The stations were located at the north-eastern edge of the Adriatic microplate. The knowledge of the crustal structure under Istra will help the understanding of the tectonic evolution within the broader region of the contact between Adria and Eurasia. Teleseismic data recorded at three-component stations were analyzed using the *P* receiver functions method, which allows detecting seismic discontinuities within the crust and upper mantle below the stations. To determine more detailed crustal structure, we have done 1-D forward modelling of receiver functions. The results of modelling are the *S*-wave velocity models of the crust beneath the stations. Calculated receiver functions showed three converted phases in the first 5 s of delay time, thus suggesting three seismic discontinuities in the crust, that is, discontinuity in the shallowest part of the upper crust, intracrustal discontinuity, and the Mohorovičić discontinuity. A forward modelling approach at all three stations showed a shallow high-velocity zone observed at a depth between 2 and 8 km. This zone may probably be related to an anhydrite series with dolomite alternations characterised by high seismic velocity. Intracrustal discontinuity is defined at a depth between 18 and 21 km. Models of the shear velocity at the three stations show a decreasing of the Moho depth from 43 km at the northern Istra to 37 km at the south-eastern part of Istra.

Keywords: Istra, crustal structure, *P* receiver function, forward modelling

1. Introduction

The current article is based on the results of the recent passive seismic experiment ALPASS-DIPS (**A**lpine **L**ithosphere and Upper Mantle **PAS**sive **S**eismic Monitoring – **DI**narides-**P**annonian **S**egment), that was part of the larger ALPASS experiment (Brückl et al., 2005). The project ALPASS-DIPS covered Istra peninsula, wide area of NW Dinarides, a transitional zone to-

wards the Pannonian basin, and the SW part of the Pannonian basin (Fig. 1). The main tectonic feature in this area is the boundary between the Adriatic microplate and the European plate. The aim of the ALPASS-DIPS project was to apply passive seismic methodology in exploring the lithospheric structures related to this zone. The study area was covered by fifteen temporary seismic stations (Fig. 1). Most of the seismic stations were deployed along the profile stretching from Istra to the Drava River at the Hungarian-Croatian border. We will focus here on three stations deployed in Istra and named Cro_01, Cro_13, and Cro_14 (Fig. 1). Teleseismic data recorded at temporary seismic stations during 15 months will be used to characterize the structure of the crust beneath Istra and the depth of Mohorovičić discontinuity, or Moho in abbreviated form (Mohorovičić, 1910).

    Lithospheric velocity structure of the study area has been recently imaged to a depth of about 50 km as a part of a wide-angle refraction and reflection experiment ALP 2002 (Brückl et al., 2003). The study area in Istra is crossed in the N–S direction by the termination of the Alp01 profile (Fig. 1). It is about a 600-km-long profile that crosses the Alpine orogen and the contact between the European plate and the Adriatic microplate. The resulting velocity model along the Alp01 profile shows that the European Moho dips to the south at a maximum depth of 47 km below the transition from the Eastern to the South-
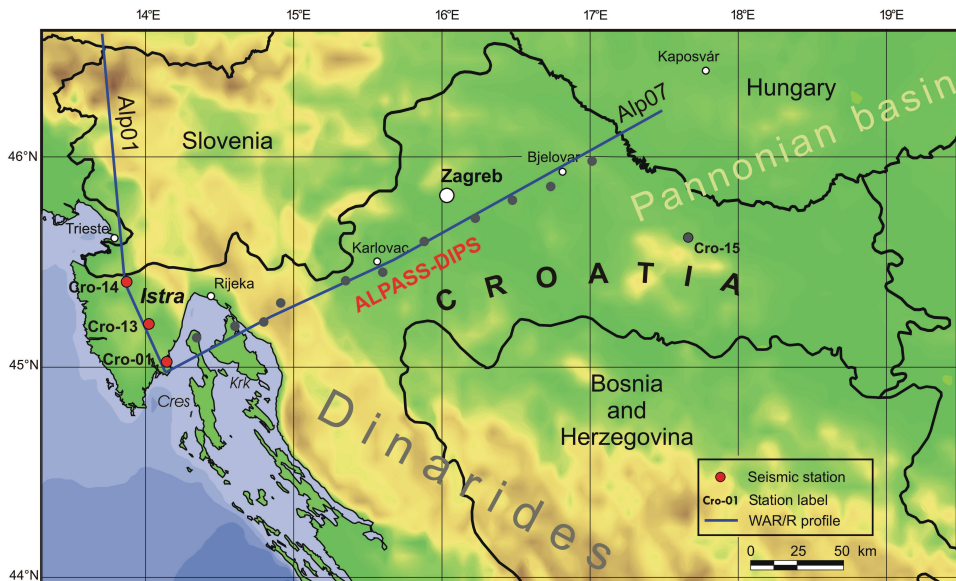
Figure 1. Locations of temporary seismic stations in Istra (Cro_01, Cro_13 and Cro_14) are denoted with red circles. The black dots are the other temporary stations deployed within the ALPASS-DIPS experiment. Alp01 and Alp07 are active source refraction and wide-angle reflection (WAR/R) profiles from the ALP 2002 project.

ern Alps (Brückl et al., 2007). At the southern end of the profile (Istra), there is a very sharp shallowing of the Moho with a decrease in depth from 40 to 28 km. The upper crust under the External Dinarides and the Adriatic foreland is characterised by a high-velocity layer, with velocities of about 6.2 km/s near surface and about 6.4 km/s at a depth of 6 km. The termination of the Alp01 profile is crossed by the beginning of the Alp07 profile, also from the ALP 2002 project (Fig. 1). It stretches in the SW–NE direction, from the Istra peninsula to the SW part of the Pannonian basin. The Mohorovičić discontinuity at the SW end of the profile is at a depth of 28 km with increasing depth under the Dinarides (Šumanovac et al., 2009). The velocity in the upper crust at the SW end of the Alp07 profile also indicates a high-velocity layer to a depth of about 5 km.

A recent receiver function study in the External Dinarides (Stipčević et al., 2011) suggests that the Moho depth is in the range from around 40 km for the Northern Adriatic to more than 55 km for the central part of the External Dinarides. A map of the Moho compiled from a receiver function study together with results from Grad et al. (2009) shows the Moho depth in Istra from 40 km in the northern part to about 33 km at the southern end. This is broadly in line with other maps of the Moho depth in Europe (e.g. Ziegler and Dézes, 2006; Tesauro et al., 2008).

In this article, crustal structure is derived from a passive seismic experiment. The teleseismic events recorded at three temporary stations have been analysed by the receiver function method. This method gives the estimate of the major velocity discontinuities by *Ps* conversions. The 1-D forward modelling of receiver functions was used to construct crustal shear-velocity models under the three stations in Istra.

2. Geological setting

The temporary seismic stations (Cro_01, Cro_13, and Cro_14) are located at the boundary between the Adriatic microplate and the European plate in the region of Northern Adriatic (Fig. 2). The area is characterised by active convergence and the movement of the Adriatic microplate to the north-northeast (Grenerczy et al., 2005), with the counter-clockwise rotation around the pole that is located in the western Alps (Anderson and Jackson, 1987; Weber et al., 2010). As a result of pushing by the African plate, the Adriatic microplate is thrust into the European continent, thus causing the Earth's crust deformation concentrated in the Alpine-Dinaric orogen. Until the 90s, the Adriatic microplate was considered unique, with no significant seismic activity (Anderson and Jackson, 1987). The present-day kinematics and deformation are reasonably well known because of the large number of GPS measurements covering the area of the Adriatic microplate. According to results based on GPS measurements (Oldow et al., 2002) and seismic activity in the central part of

the Adriatic Sea, it is assumed that the Adriatic microplate is not unique, but consists of two segments: northern and southern (Console et al., 1993; Ivančić et al., 2006). The boundary between them extends approximately from Garga-no, on the southeast coast of Italy, to Dubrovnik (Westaway, 1990). The south-ern block has the opposite rotation to the northern part (Favali et al., 1990; D'Agostino et al., 2008). Recent studies in this area based on deep refraction and wide angle-reflection experiment support the idea of subduction of the Eu-ropean plate below the Adriatic microplate in the area of the Southern Alps (Brückl et al., 2007). Consistent with this concept is also a tomographic model of the upper mantle under the Eastern Alps and the transition to the Panno-nian realm based on the ALPASS teleseismic experiment (Mitterbauer et al., 2011). At the same time, underthrusting of the Adriatic microplate beneath the Dinarides is substantiated by results of the deep refraction experiment (Šumanovac et al., 2009) and gravity modelling (Šumanovac, 2010).

The Istra peninsula, in which all the three stations are located, belongs to the northwestern part of the former Adriatic carbonate platform (AdCP), which existed from the Middle Permian to Eocene, with the thickness of car-bonate sediments greater than 3500 m (Vlahović et al., 2005). Eocene forami-niferal limestones, transitional beds, and flysch lie on the carbonate platform sediments. According to the geological map, station Cro_13 is located on Eoce-
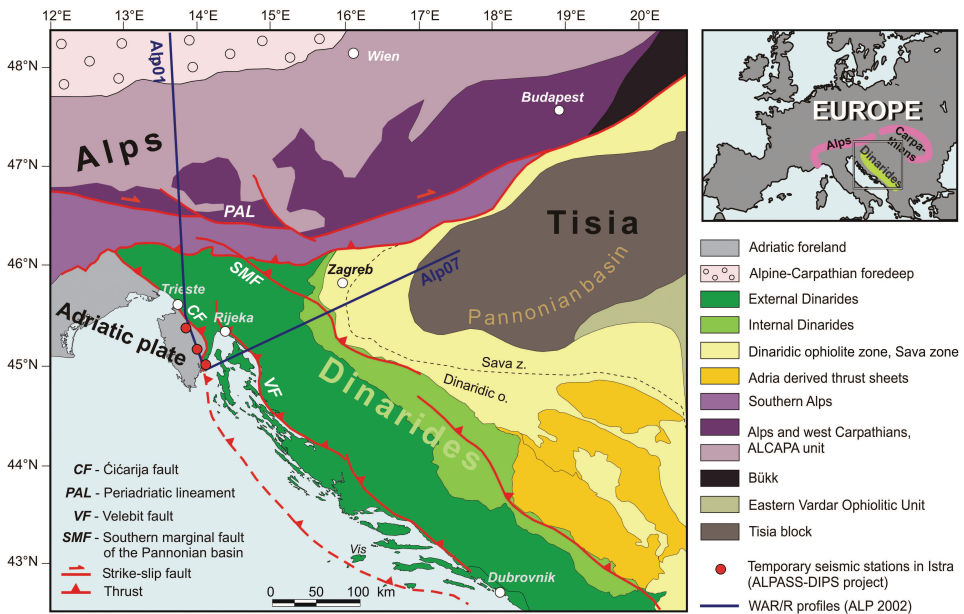

Figure 2. Geology and tectonics in the wider area. Red circles indicate temporary seismic stations in Istra and blue lines are two refraction and wide-angle reflection (WAR/R) profiles from the ALP 2002 experiment (generalized after Schmid et al., 2008).

ne sandstones and marls, whereas stations Cro_01 and Cro_14 are situated on Upper Cretaceous limestones (Geological Map of the Republic of Croatia, 2009).

3. Data and method of analysis

The teleseismic events used in this study have been collected from the passive seismic experiment ALPASS-DIPS. The APASS-DIPS project consisted of fifteen temporary seismic stations; but for this study, we have selected three stations located in Istra: Cro_01, Cro_13, and Cro_14 (Fig. 1). The earthquakes were recorded on three-component short-period seismic stations. The seismometers used were 2 Hz MARK L4-1D and ELGI-DAS data logger. The data were recorded during the period of 15 months, from November 2005 to January 2007. From recorded earthquakes, we have selected 34 teleseismic events within epicentral distance between 30° and 90° (Fig. 3) and with a magnitude greater than 5.5. For the receiver function analysis, we had to remove data with low signal-to-noise ratio; and finally, sixteen events per station were used. Most of the selected events are located to the north and east from the stations, with back azimuths between 0° and 100° (Fig. 3); only a number of events originate from the south and west.
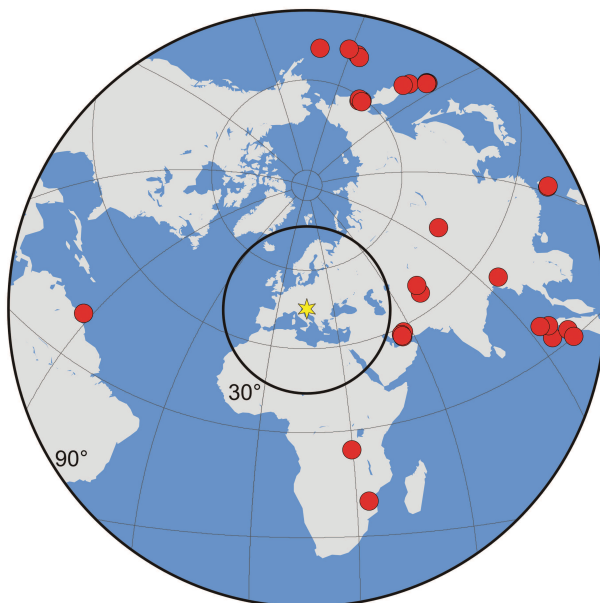
Figure 3. Distribution of teleseismic events (red circles) recorded by four stations (Cro_1, Cro_13, Cro_14) within ALPASS-DIPS project. Selected events are with epicentral distance between 30° and 90°. The star marks position of the ALPASS-DIPS project.

Receiver functions are calculated using the approach of Kind et al. (1995) and Yuan et al. (1997). The *P* receiver function method is based on the analysis of converted *P*-to-*S* phase contained in the *P*-wave coda. The method is used to separate the response of the Earth's structure near the receiver from other influences such as the source and ray path through the mantle (Langston, 1979; Owens et al., 1984; Kind and Vinnik, 1988; Kosarev et al., 1999). *P*-to-*S* conversions are generated at significant velocity discontinuities in the crust and upper mantle beneath a seismic station, where *P* waves are partly converted to *S* waves. *Ps* phases travel the last part of their path with shear velocity. The delay time of the converted *Ps* phase relative to the arrival time of the direct *P* wave depends on the depth of the discontinuity, the ray parameter of the incident *P* wave, and the *P* and *S* velocities in the layers. By extracting *Ps* phases from the *P*-wave coda, we can acquire information about the velocity structure beneath the recording site. The seismometers at seismic stations are oriented in the *ZNE* coordinate system, and most of the *Ps* converted energy is contained in the horizontal components. Rotation of the *ZNE* component waveforms into the local *P-SV-SH* ray-based coordinate system isolates the *Ps* converted phases in the *SV* component, which is perpendicular to the direction of the *P* component containing the *P*-wave motion. The influences of the travel path effects and source parameter are removed by deconvolution of the *P* component from the *SV* component. The *SV* component is called *receiver function*. The final *P* receiver function contains, in addition to the primary converted phases, multiple reflections and conversions generated between velocity discontinuities in the crust and the Earth's surface.

Pre-processing of the selected teleseismic data consisted of cutting each waveform to a 150 s long window, 50 s before *P*-wave arrival, and 100 s after. The data were first filtered with Butterworth bandpass filter between 0.1 and 1 Hz. The rotation to *P-SV-SH* coordinate system was based on theoretical back azimuth and incidence angle.

Receiver functions obtained for different events at each station are stacked to improve the signal-to-noise ratio. Calculated receiver functions should be equalized for the epicentral distances and ray paths (moveout correction) in order to obtain the constructive interference of stacked traces. With regard to epicentral distances ($>30°$), it is acceptable to approximate the incoming *P* waves as plane waves. The delay times of *Ps* conversions of all receiver functions have been adjusted with regard to the arrival time of the *Ps* phase at a reference epicentral distance of 67° (ray parameter of 6.4 sec/°, Yuan et al., 1997). The velocity model used is IASP91, a global one-dimensional velocity model (Kennett and Engdahl, 1991).

The analysis of receiver functions is here focused on information about the depth of the Mohorovičić discontinuity and velocity discontinuities within the crust. Forward modelling of receiver functions has been used to obtain the shear-velocity structure of the crust beneath each station.
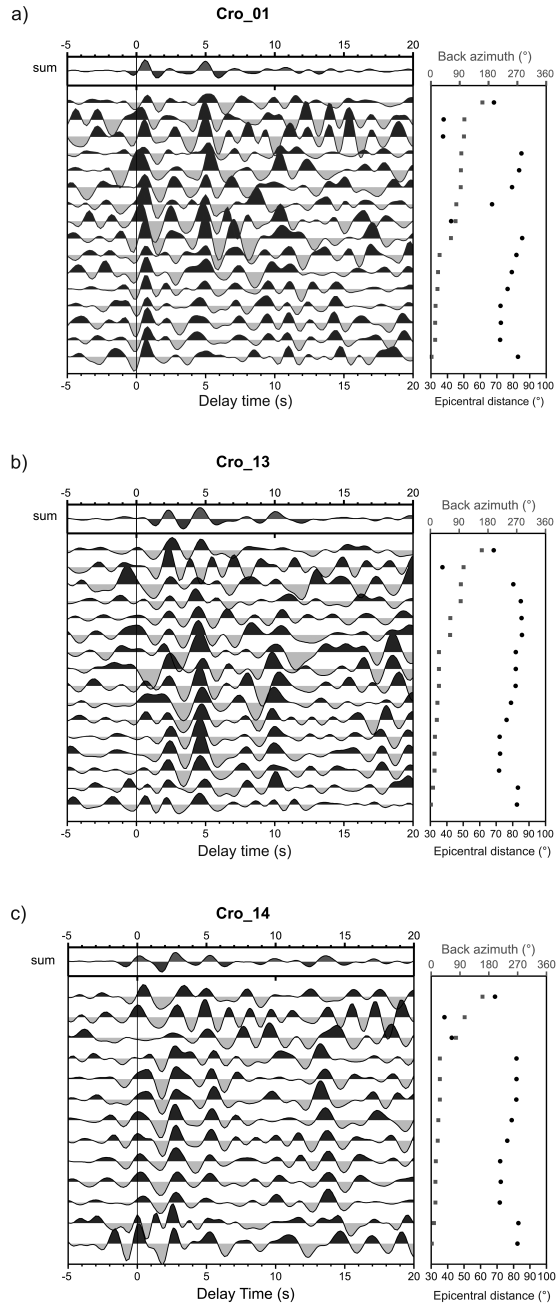
4. Observed receiver functions

The distance-corrected, individual *P* receiver functions calculated for the three stations in Istra (Cro_01, Cro_13, and Cro_14) are summed and presented in Figs 4a–4c. The traces are arranged with increasing back azimuth. Positive amplitudes (black) indicate a velocity increasing with depth, whereas negative amplitudes (gray) indicate a velocity decreasing with depth. Zero time corresponds to direct *P*-wave arrival. All the three stations obtained good Moho conversions, although short-period seismometers were used.

The receiver functions for the stations in Istra show a similar waveform with three main positive amplitudes in the first 6 s. The first amplitude is observed between 0 and 0.5 s after the direct *P*-wave arrival with the greatest amplitude at station Cro_01 (Fig. 4a). This shallowest converted phase originates from discontinuity in the upper crust. Positive amplitude indicates a velocity increase with depth, so most probably it originates from the high-velocity layer in the upper 5 to 6 km observed under the Istra near the intersection of Alp07 and Alp01 profiles (Brückl et al., 2007; Šumanovac et al., 2009). The origin of this amplitude will be confirmed by the forward modelling of receiver functions in the next chapter.

A conversion with positive polarity between 2 and 3 s can be seen at all stations. The amplitude of this phase is strong at stations Cro_13 and Cro_14 (Figs 4b and c), whereas it is rather weak at the stacked trace of the Cro_01 station (Fig. 4a). However, the amplitude is rather strong on some individual traces of station Cro_01. The conversion observed in the time interval between 2 and 3 s most probably originates from discontinuity at the boundary between the upper and lower crust. However, the presence of strong, shallow discontinuities or significant sedimentary cover may cause large-amplitude reverberations masking the primary *Ps* converted phases and making the estimation of the discontinuity depth difficult (Geissler et al., 2005; van der Meijde et al., 2003). The converted phase from the Moho arrives at delay time between 4.6 and 5.2 s, depending on the station. The *Ps* delay time indicates the shallowest Moho at station Cro_13 (Fig. 4b), and the deepest Moho at station Cro_14 (Fig. 4c).
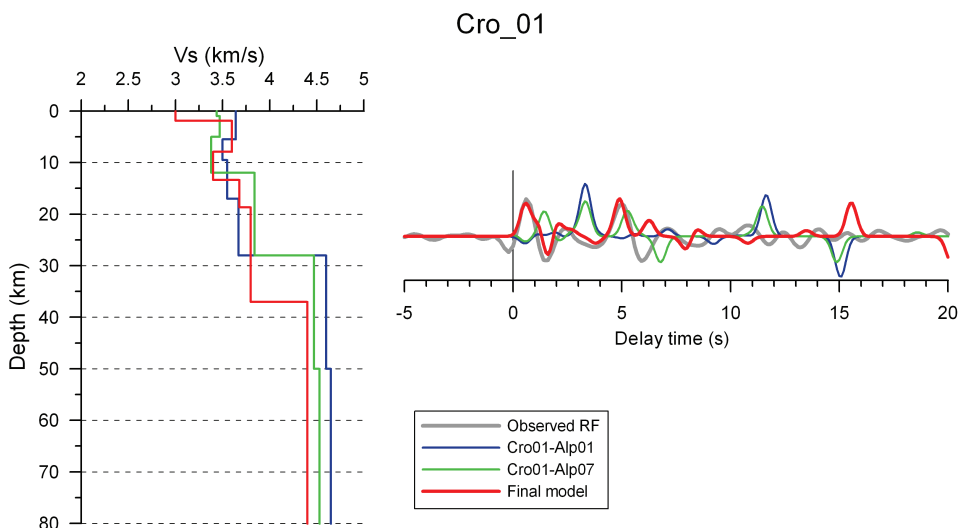
5. Receiver function modelling

The main goal of forward modelling was to construct a relatively simple model that can describe well the main phases in the observed receiver function. The synthetic receiver functions were calculated by using the code of Frederiksen and Bostock (2000). Models consisted of homogeneous isotropic layers above the half space, with boundaries that were parallel to the surface. Each layer was defined according to its thickness, *S*-wave velocity, *P*-wave velocity, and density.

Figure 4. Receiver functions for stations in Istra: (a) Cro_01, (b) Cro_13 and (c) Cro_14. Individual traces are arranged with increasing back azimuth (rectangles). Epicentral distances are indicated with black dots. Stacked trace for all events is shown at the top.

Temporary seismic stations Cro_13 and Cro_14 are located in Istra, at the end of the profile Alp01 from the ALP 2002 experiment (Fig. 1). Therefore, the initial velocity models under both stations are extracted from the *P*-wave velocity model along the Alp01 profile (Brückl et al., 2007). Station Cro_01 is located near the intersection of the Alp07 and the Alp01 profiles (Fig. 1), so the initial 1-D models are derived from both *P*-wave velocity models. The velocity models are smoothed to consist of four to five layers over a half space in the mantle. The *S*-wave velocities were calculated from the V_p with the assumed V_p/V_s ratio of 1.726 in the upper crust, 1.74 in the lower crust, and 1.79 in the mantle (Kennett and Engdahl, 1991). Based on the given model, receiver functions were calculated for the converted *Ps* phases and their multiples of the first order. The rotation was done to the *P-SV-SH* coordinate system, so that the receiver function component consists of mainly *SV* energy. Due to the rotation in the ray-based coordinate system, the receiver function does not contain the direct *P* wave, but the first amplitude corresponds to a shallow discontinuity. Synthetic receiver function was then compared with the stacked trace for each station.

At station Cro_01, both the initial models could not explain well the observed receiver function. Calculated receiver function from the Alp01 and Alp07 velocity models give the *Ps* phase from the Moho about 1.5 s earlier than the observed receiver function (Fig. 5), indicating that the crustal thickness is greater. According to the amplitude size, velocity contrast at the Moho is well


Figure 5. Results of the modelling for station in Istra, Cro_01. The initial velocity models were extracted from the *P*-wave velocity model along the Alp01 profile (blue line) and Alp07 profile (green line). The best fitting synthetic receiver function is shown with red line.

defined in the Alp07 profile. The observed receiver function shows a strong phase in the first second that can be attributed to a significant velocity increase near the surface. High velocity layer (HVL) at less than 5 km depth is also defined in the deep seismic refraction profiles Alp01 and Alp07. A much better fit to the observed receiver function is obtained for the model with a stronger velocity increase at about 2 km depth (Fig. 5; red line) followed by 6 km thick HVL (V_s = 3.6 km/s). Below this layer, velocity decreases, and it is rather low until the boundary between the lower crust and the upper crust (~19 km). The shear-velocity structure defined by the final model shows the main velocity contrast at a depth of 37 km, which can be interpreted as the Mohorovičić discontinuity.

According to the initial model under station Cro_13 (Fig. 6a; blue line), velocity is high in the shallowest part of the upper crust (to a depth of 6 km). The high-velocity anomaly is followed by a lower velocity (V_p < 6.20 km/s), which extends to a depth of 18 km. The Mohorovičić discontinuity is located at a significantly shallower depth (~28 km) as compared with the rest of the Alp01 profile. Synthetic receiver function is first calculated for the initial model. It shows that the *Ps* phase converted at the Mohorovičić discontinuity comes much earlier than in the observed receiver function; and based on amplitude value, the velocity contrast is very high (Fig. 6a). Discrepancy also exists with regard to the converted *Ps* phases on the intracrustal discontinuity. The amplitudes calculated from the Alp01 model are very low, and delay times do not match the observed receiver function. It was necessary to adjust the velocity model to obtain a better fit of the synthetic and observed receiver functions.

The initial model was changed with a high-velocity layer at a depth between 2.2 and 8.2 km (V_s = 3.65 km/s) followed by a lower velocity than had been defined in the Alp01 model. In this way, the velocity contrast at the interface between the upper and lower crust was greater. The Moho depth in the new model was considerably changed, to a depth of 40 km (Fig. 6a; red line). The high-velocity layer is 6 km thick, the same as at the station Cro_01. An attempt to decrease its thickness to 4 km results in a misfit between the synthetic and observed receiver functions (Fig. 6b; green line). Synthetic receiver function shows additional amplitude at approximately 3 s delay time, which is not visible in the observed receiver function. Unsatisfying results are also obtained for a model with thinner HVL at a greater depth, between 3.2 and 7.2 km (Fig. 6b; purple line).

The initial 1-D model under station Cro_14 was also constructed from the *P*-wave velocity model along the Alp01 profile; and in the upper crust, it demonstrated similar features to the model under station Cro_13 (Fig. 7a; blue line). However, the thickness of the lower crust is greater under station Cro_14, and Mohorovičić discontinuity is situated much deeper, at a depth of 40 km. The synthetic receiver function obtained from this model shows very small amplitudes of the *Ps* phases that originate from the interfaces in the crust than on the observed receiver function (Fig. 7a). In contrast, the synthetic receiver
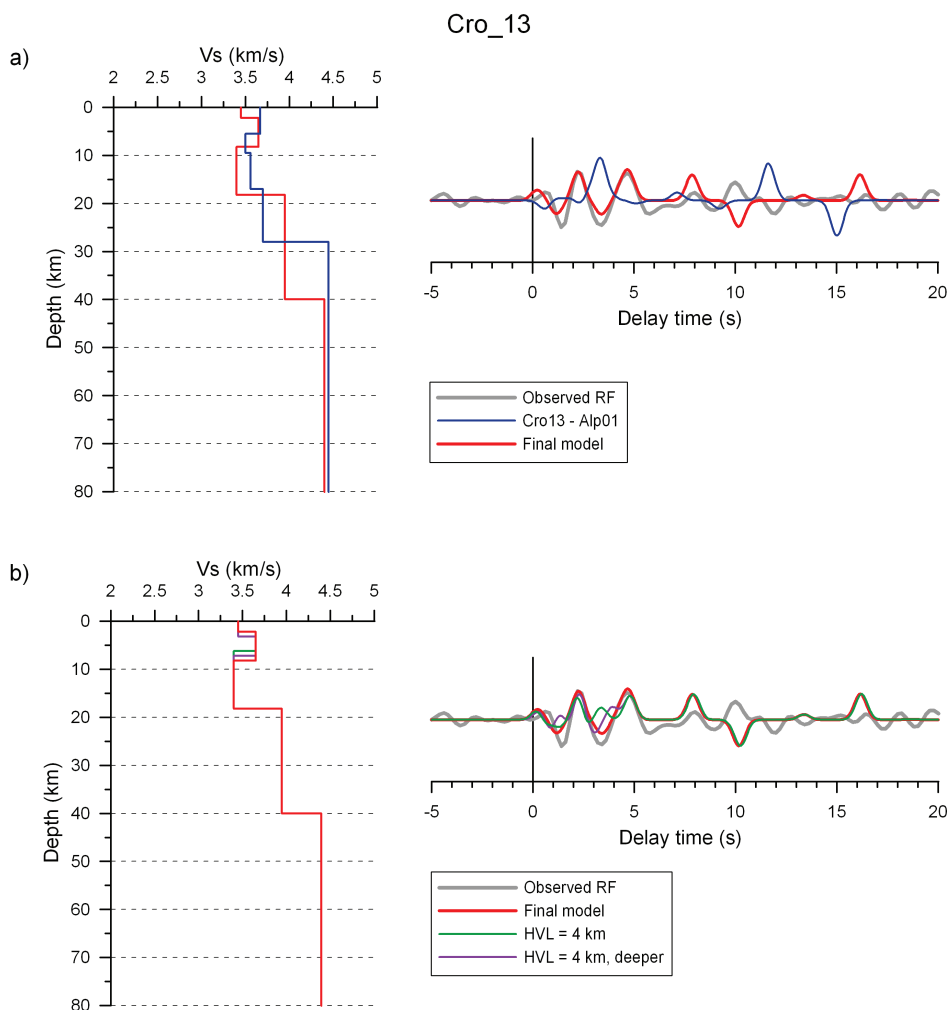
Figure 6. Forward modelling of the receiver function at station Cro_13: (a) for the initial model from Alp01 profile (blue line) and final model (red line); (b) models with smaller thickness of the high-velocity layer: with the same depth of the top of the HVL (green) and with the greater depth of the top (purple).

function shows stronger amplitude of the *Ps* phase from the Moho. This indicates a too large velocity contrast at the crust-mantle boundary in the initial model. The difference in the delay time of the *Ps* phase from the Moho is not as great as for station Cro_13, which means that the Moho depth in the model is better defined. A good fit to the observed data was obtained for the model with intracrustal discontinuity at a depth of 20 km, but with very strong velocity contrast (V_s = 3.27 to 4.0 km/s) needed to satisfy the strong amplitude with
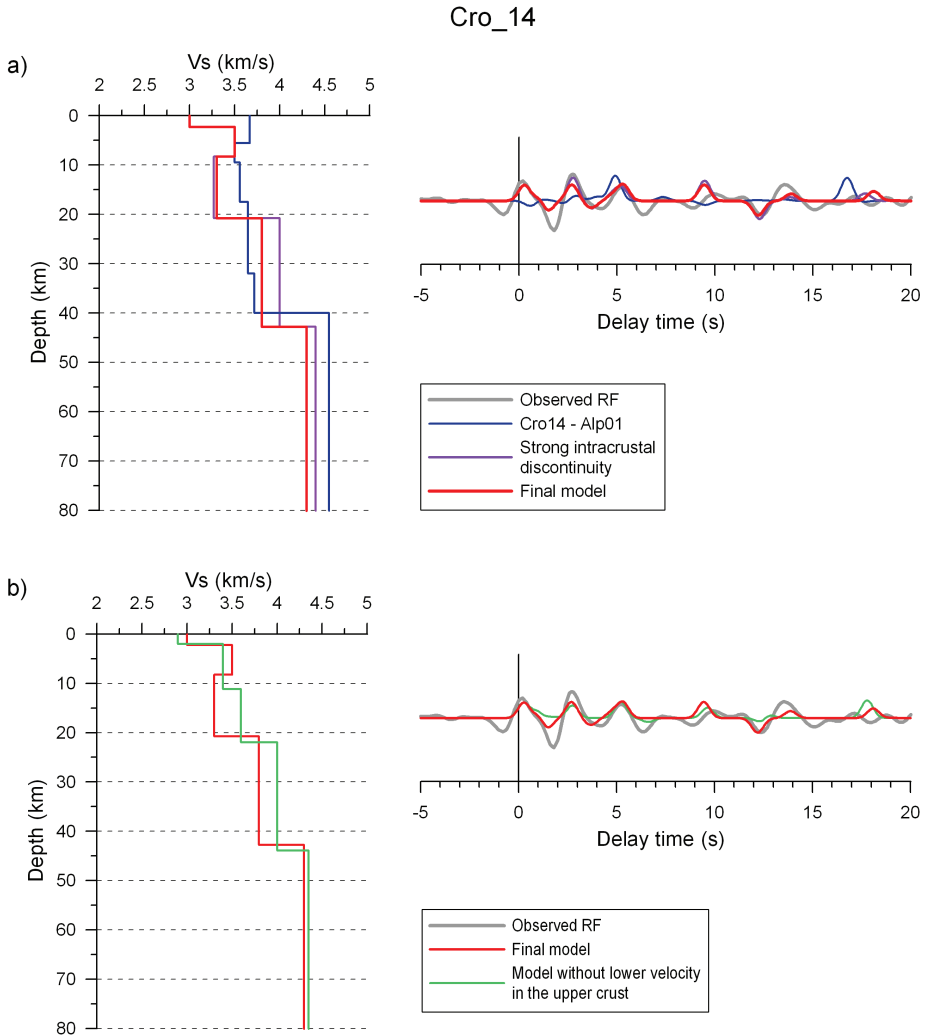
Cro_14

Figure 7. Forward modelling of the receiver function at station Cro_14: (a) for the initial model from Alp01 profile (blue line), model with strong intracrustal discontinuity which fits well the observed receiver function (purple line) and final model (red line); (b) comparison of a model without velocity decrease in the upper crust (green) with the final model (red).

delay time about 3 s (Fig. 7a, purple line). However, the velocity contrast seemed to be unrealistic; so, the modelling was done with a smaller velocity in the lower crust (Fig. 7, red line). The refraction model of the Alp01 profile also does not show significant velocity contrast within the crust.

The example of the crustal velocity model under the station Cro_14 also shows the need for high velocity in the shallowest part followed by the lower

velocity (Fig. 7b). The shear velocity model with a gradual increase in velocity within the crust gives the unsatisfying fit between the observed and synthetic receiver function (Fig. 7b; green line).

6. Discussion and conclusions

The teleseismic data recorded at three temporary seismic stations in Istra, within the ALPASS-DIPS experiment, were analysed by the *P* receiver function method. Calculated receiver functions pointed to the main characteristics of the Earth's crust in Istra, but a more precise crustal structure beneath the three stations has been estimated by 1-D forward modelling. The resulting crustal models are presented as *S*-wave velocity models.

Shear-velocity structures obtained from 1-D forward modelling include significant velocity contrast at the depth of 2–3 km, for all the three stations in Istra (Fig. 8). This shallow velocity discontinuity was required to fit the observed receiver functions. High-velocity structure in the uppermost 5 km is also present in the models based on deep seismic refraction profiles in Istra (Brückl et al., 2007; Šumanovac et al., 2009). Exploration boreholes in this area drilled for oil and gas prospecting found anhydrite/gypsum series as well as alternations of dolomitic limestones with anhydrite which have rather high seismic velocities (Sheriff and Geldart, 1995). In line with the deep seismic refraction survey and well-logging data, shallow high-velocity structure may be attributed to the carbonate platform sediments i.e. the anhydrite series.

At stations Cro_13 and Cro_14, there are strong phases between 2 and 3 s delay time; in other words, between the shallow high-velocity structure and
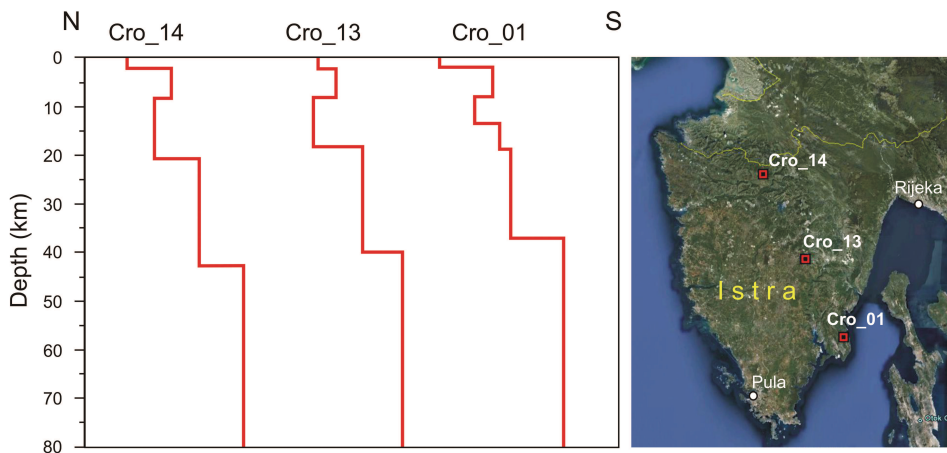
Figure 8. Final models of the S wave velocity structures beneath three stations in Istra ploted in the north-south direction. Locations of the stations are marked on the map (right) with red rectangles.

the Moho. This phase can be attributed to *Ps* conversion from intracrustal velocity. To fit the observed phases, velocity models were defined with rather strong velocity discontinuity at approximately 20 km depth (Fig. 8). The southern part of the deep seismic refraction profile Alp01 does not contain such a large intracrustal discontinuity, but the Moho depth under station Cro_13 is defined at 28 km (Brückl et al., 2007). There is still a possibility that these phases could be stronger because of the influence of multiples from the near-surface structures. This could be true for station Cro_14 with a strong velocity increase in the shallowest part, but the model of station Cro_13 does not include such a strong, shallow velocity contrast. The *S*-velocity crustal structure is in good agreement with the receiver function study of Stipčević et al. (2011) at the station located near Rijeka (Northern Adriatic, Fig. 1). They reported a two-layered crust with a 3 km-thick low-velocity layer above the upper crust and rather high velocities in the upper crust.

The results of the 1-D forward modelling at the stations in Istra reveal crustal thicknesses between 37 and 43 km that decrease from north to south (Fig. 8). The Moho depth obtained from receiver functions for stations Cro_01 and Cro_13 is significantly greater than the one from the deep seismic refraction experiment. It should be noted that these stations are at the very end of the Alp01 profile, where ray coverage is much lower than the rest of the profile. The difference in Moho depth, but only partly, could be caused by different methods that sample the boundaries in different places. Shallower Moho from receiver function modelling could be obtained if lower S wave velocity is considered in the crust. By considering higher values of the V_p/V_s the interface would be shallower. If V_p/V_s of 1.8 instead of 1.76 was applied in the lower crust under the station Cro_13, we could get the depth of the Moho about 3 km shallower.

Crustal thickness in Istra obtained by receiver function forward modelling is in accordance with the known relationships of the Mohorovičić discontinuity depth in the area of Northern Adriatic (Aljinović, 1987; Ziegler and Dézes, 2006; Tesauro et al., 2008; Grad et al., 2009), but the difference in the absolute Moho depth is between 2 and 5 km.

References

Aljinović, B. (1987): On certain characteristics of the Mohorovičić discontinuity in the region of Yugoslavia, *Acta Geol.*, **17**, 13–20.

Anderson, H. and Jackson, J. (1987): Active tectonics of the Adriatic region, *Geophys. J. Int.*, **91**, 937–983, DOI: 10.1111/j.1365-246X.1987.tb01675.x.

Brückl, E., Behm, M., Grad, M., Guterch, A., Hegedűs, E., Keller, G. R., Kominaho, K., Kovacs, A., Kozlovskaya, E., Lambrecht, A., Mitterbauer, U., Orešković, J., Rumpfhuber, E., Šumanovac, F., Tiira, T., Velasco, A., Wilde-Piorko, M. and ALPASS Working Group (2005): ALPASS – Passive seismic monitoring in the Eastern Alps, *Eos Trans. AGU*, **86**(52), Fall Meet. Suppl., Abstract S41A-0974.

Brückl, E., Bleibinhaus, F., Gosar, A., Grad, M., Guterch, A., Hrubcová, P., Keller, G. R., Šumanovac, F., Tiira, T., Yliniemi, J., Hegedűs, E. and Thybo, H. (2007): Crustal structure due to collisional and escape tectonics in the Eastern Alps region based on profiles Alp01 and Alp02 from the ALP 2002 seismic experiment, *J. Geophys. Res.*, **112**, B06308, DOI: 10.1029/2006JB004687.

Brückl, E., Bodoky, T., Hegedűs, E., Hrubcová, P., Gosar, A., Grad, M., Guterch, A., Hajnal, Z., Keller, G. R., Špicak, A., Šumanovac, F., Thybo, H., Weber, F. and ALP 2002 Working Group (2003): ALP 2002 Seismic Experiment, *Stud. Geophys. Geod.*, **47**, 651–657.

Console, R., Di Giovambattista, R., Favali, P., Presgrave, B. W. and Smriglio, G. (1993): Seismicity of the Adriatic microplate, *Tectonophysics*, **218**, 343–354.

D'Agostino, N., Avallone, A., Cheloni, D., D'Anastasio, E., Mantenuto, S. and Selvaggi, G. (2008): Active tectonics of the Adriatic region from GPS and earthquake slip vectors, *J. Geophys. Res.*, **113**, B12413, DOI: 10.1029/2008JB005860.

Frederiksen, A. W. and Bostock, M. G. (2000): Modelling teleseismic waves in dipping anisotropic structures, *Geophys. J. Int.*, **141**, 401–412, DOI: 10.1111/j.1365-246X.2009.04115.x.

Favali, P., Mele, G. and Mattietti, G. (1990): Contribution to the study of the Apulian microplate geodynamics, *Mem. Soc. Geol. It.*, **44**, 71–80.

Geissler, W. H., Kämpf, H., Kind, R., Klinge, K., Plenefisch, T., Horálek, J., Zedník, J. and Nehybka, V. (2005): Seismic structure and location of a CO2 source in the upper mantle of the western Eger (Ohře) Rift, central Europe, *Tectonics*, **24**, TC5001, DOI: 10.1029/2004TC001672.

Geological Map of the Republic of Croatia (2009): Geološka karta Republike Hrvatske, 1:300.000, Croatian Geological Survey, Zagreb.

Grad, M., Tiira, T. and ESC Working Group (2009): The Moho depth map of the European Plate, *Geophys. J. Int.*, **176**, 279–292.

Grenerczy, G., Sella, G., Stein, S. and Kenyeres, A. (2005): Tectonic implications of the GPS velocity field in the northern Adriatic region, *Geophys. Res. Lett.*, **32**, L16311, DOI: 10.1029/2005GL022947.

Ivančić, I., Herak, D., Markušić, S., Sović, I. and Herak, M. (2006): Seismicity of Croatia in the period 2002–2005, *Geofizika*, **23**, 87–103.

Kennett, B. L. N. and Engdahl, E. R. (1991): Traveltimes for global earthquake location and phase identification, *Geophys. J. Int.*, 105, 429–465, DOI: 10.1111/j.1365-246X.1991.tb06724.x.

Kind, R., Kosarev, G. L and Petersen, N. V. (1995): Receiver functions of the stations of the German regional Seismic Network (GRSN), *Geophys. J. Int.*, **121**, 191–202.

Kind, R., and Vinnik, L. P. (1988): The upper mantle discontinuities underneath the GRF array from P-to-S converted phases, *J. Geophys.*, **62**, 138–147.

Kosarev, G., Kind, R., Sobolev, S. V., Yuan, X., Hanka, W. and Oreshin, S. (1999): Seismic evidence for a detached Indian lithosphere mantle beneath Tibet, *Science*, **283**, 1306–1309.

Langston, C. A. (1979): Structure under Mount Rainier, Washington, inferred from teleseismic body waves, *J. Geophys. Res.*, **84**, 4749–4762.

Mitterbauer, U., Behm, M., Brückl, E., Lippitsch, R., Guterch, A., Keller, G. R., Koslovskaya, E., Rumpfhuber, E. M. and Šumanovac, F. (2011): Shape and origin of the East-Alpine slab constrained by the ALPASS teleseismic model, *Tectonophysics*, **510**, 195–206.

Mohorovičić, A. (1910): Potres od 8. X 1909. (Das Beben vom 8. X. 1909.), Godišnje izvješće Zagrebačkog meteorološkog opservatorija za godinu 1909. (Jahrbuch des meteorologischen Observatoriums in Zagreb (Agram) für das Jahr 1909), **9**(4), 1–56 (and English translation in 1992: Earthquake of 8 October 1909, *Geofizika*, **9**, 3–55).

Oldow, J. S., Ferranti, L., Lewis, D. S., Campbell, J. K., D'Argennio, B., Catalano, R., Pappone, G., Carmignani, L., Conti, P. and Aiken, C. L. V. (2002): Active fragmentation of Adria, the North African promontory, central Mediterranean orogen, *Geology*, **30**, 779–782.

Owens, T. J., Zandt, G. and Taylor, S. R. (1984): Seismic evidence for an ancient rift beneath the Cumberland Plateau, Tennessee: A detailed analysis of broadband teleseismic *P* waveforms, *J. Geophys. Res.*, **89**, 7783–7795.

Schmid, S. M., Bernoulli, D., Fügenschuh, B., Matenco, L., Schefer, S., Schuster, R., Tischler, M. and Ustaszewski, K. (2008): The Alpine–Carpathian–Dinaridic orogenic system: correlation and evolution of tectonic units. *Swiss J. Geosci.*, **101**, 139–183.

Sheriff, R. E. and Geldart, L. P. (1995): *Exploration seismology*. Second Edition, Cambridge Univ. Press, Cambridge, 592 pp.

Stipčević, J., Tkalčić, H., Herak, M., Markušić, S. and Herak, D. (2011): Crustal and uppermost mantle structure beneath the External Dinarides, Croatia, determined from teleseismic receiver functions, *Geophys. J. Int.*, **185**, 1103–1119, DOI: 10.1111/j.1365-246X.2011.05004.x.

Šumanovac, F. (2010): Lithosphere structure at the contact of the Adriatic microplate and the Pannonian segment based on the gravity modelling, *Tectonophysics*, **485**, 94–106, DOI: 10.1016/j.tecto.2009.12.005.

Šumanovac, F., Orešković, J., Grad, M. and ALP 2002 Working Group (2009): Crustal structure at the contact of the Dinarides and Pannonian basin based on 2-D seismic and gravity interpretation of the Alp07 profile in the ALP 2002 experiment, *Geophys. J. Int.*, **179**, 615–633, DOI: 10.1111/j.1365-246X.2009.04288.x.

Tesauro, M., Kaban, M. K. and Cloetingh, S. A. P. L. (2008): EuCRUST-07: A new reference model for European crust, *Geophys. Res. Lett.*, **35**, 5313–5318, DOI: 10.1029/2007GL032244.

Van der Meijde, M., van der Lee, S. and Giardini, D. (2003): Crustal structure beneath broad-band seismic stations in the Mediterranean region, *Geophys. J. Int.*, **152**, 729–739.

Vlahović, I., Tišljar, J., Velić, I. and Matičec, D. (2005): Evolution of the Adriatic Carbonate Platform: Palaeogeography, main events and depositional dynamics, *Palaeogeogr. Palaeoclimatol. Palaeoecol.*, **220**, 333–360.

Weber, J., Vrabec, M., Pavlovčič-Prešeren, P., Dixon, T., Jiang, Y. and Stopar, B. (2010): GPS-derived motion of the Adriatic microplate from Istria Peninsula and Po Plain sites, and geodynamic implications, *Tectonophysics*, **483**, 214–222.

Westaway, R. (1990): Present-day kinematics of the plate boundary zone between Africa and Europe, from the Azores to Aegean, *Earth Planet. Sci. Lett.*, **96**, 393–406.

Yuan, X., Ni, J., Kind, R., Mechie, J. and Sandvol, E. (1997): Lithospheric and upper mantle structure of southern Tibet from a seismological passive source experiment, *J. Geophys. Res.*, **102**, 27491–27500.

Ziegler, P. A. and Dézes, P. (2006): Crustal evolution of Western and Central Europe, *Mem. Geol. Soc. Lond.*, **32**, 43–56.

SAŽETAK

Struktura kore na području Istre određena na temelju analize funkcija prijemnika

Jasna Orešković, Franjo Šumanovac i Endre Hegedűs

Struktura Zemljine kore na području Istre određena je ispod tri privremene seizmičke stanice postavljene u okviru projekta pasivnih seizmičkih istraživanja ALPASS-DIPS (**A**lpine **L**ithosphere and Upper Mantle **PAS**sive **S**eismic Monitoring – **DI**narides--**P**annonian **S**egment). Stanice su se nalazile na sjeveroistočnom rubu Jadranske mikroploče u području sjevernog Jadrana. Nova saznanja o građi kore u Istri doprinijeti će pojašnjenju današnjih tektonskih odnosa na širem području, posebno kontaktu Jadranske mikroploče i Europske ploče. Seizmogrami dalekih potresa analizirani su metodom *P* funkcija prijemnika, koja omogućava definiranje diskontinuiteta u kori i gornjem plaštu neposredno ispod stanice. Pored funkcija prijemnika izvedeno je i jednodimenzionalno modeliranje kako bi se detaljnije definirala struktura kore. Rezultat su modeli brzina *S*-valova u kori i gornjem plaštu ispod stanica. Izračunate funkcije prijemnika na sve tri stanice pokazuju tri konvertirane faze u prvih 5 s nakon direktnog *P*-vala. One ukazuju na postojanje tri diskontinuiteta brzina u kori, i to diskontinuitet u najplićem dijelu gornje kore, diskontinuitet na granici gornje i donje kore te Mohorovičićev diskontinuitet. Rezultati modeliranja na sve tri stanice u Istri pokazuju da se na dubini između 2 i 8 km nalazi sloj velike brzine. Uzrok velikih brzina mogla bi biti karbonatna platforma, odnosno izmjene anhidrita i dolomita koji imaju velike seizmičke brzine. Granica gornje i donje kore definirana je na dubini između 18 i 20 km. Modeli brzina *S*-valova pokazuju smanjenje dubine Mohorovičićevog diskontinuiteta od 43 km u sjevernom dijelu Istre, do 37 km u jugoistočnom dijelu Istre.

Ključne riječi: Istra, struktura kore, *P* funkcije prijemnika, modeliranje

Corresponding author's address: Jasna Orešković, University of Zagreb, Faculty of Mining, Geology and Petroleum Engineering, Pierottijeva 6, HR-10000 Zagreb, Croatia, tel: +385 (0)1 5535 747, fax: +385 (0)1 5535 743, e-mail: jasna.oreskovic@rgn.hr